# Dwarf satellite galaxies in the modified dynamics

Rafael Brada and Mordehai Milgrom Condensed Matter Department, Weizmann Institute of Science, Rehovot Israel

## **ABSTRACT**

In the modified dynamics (MOND) the inner workings of dwarf satellites can be greatly affected by their mother galaxy-over and beyond its tidal effects. Because of MOND's nonlinearity a system's internal dynamics can be altered by an external field in which it is immersed (even when this field, by itself, is constant in space). As a result, the size and velocity dispersion of the satellite vary as the external field varies along its orbit. A notable outcome of this is a substantial increase in the dwarf's vulnerability to eventual tidal disruption—rather higher than Newtonian dynamics (with a dark-matter halo) would lead us to expect for a satellite with given observed parameters. The space of system parameters of the dwarf may be divided according to three main criteria: It can be either external- or internal-field dominated; it can be in the adiabatic or in the impulsive regime; and it can be in the tidal or non-tidal regime. The Milky Way's dwarf satellites populate all these regions of parameter space, and a single dwarf on an eccentric orbit can traverse several of them. The situation is particularly transparent in the external-field-dominated, adiabatic regime where the dynamics can be described analytically: due to the variation in the external-field strength with the galactocentric distance of the dwarf, R, its size changes as  $R^{-1}$ , and the internal velocities change as R. As the dwarf approaches the center it puffs up, becoming susceptible to tidal disruption. Adiabaticity is lost roughly at the same R were tidal effects become important. The behavior near and in the impulsive regime is studied numerically.

## 1. Introduction

The dynamical behavior of dwarf spheroidals and other satellites of the Milky Way holds much information pertinent to the dark-matter problem. Attempts to elicit such knowledge include, on the one hand, measurements of the satellites' intrinsic properties such as the size, luminosity, and velocity dispersion, which evince mass discrepancies in the satellites (Aaronson & Olszewski 1988, Pryor 1991, Mateo 1998). This discrepancy is removed in the modified dynamics—MOND (Milgrom 1995, McGaugh & de Blok 1998, Mateo 1998). On the other hand, the satellites can be used to probe the gravitational field of their mother galaxy (specifically, the Milky Way) by using them as test particles to probe the galaxy's potential field (e.g., Little & Tremaine 1987), or by studying tidal effects of the galaxy on the structure of the satellite taken as a finite body (e.g., Faber & Lin 1983). In Newtonian dynamics, the history of the center-of-mass motion may influence the internal workings of the satellite via tidal effects. Tidal disruption may have culled from the satellite population those that are internally weakly bound and/or move on elongated orbits, thus affecting the distribution of galactic orbits seen today (see, e.g., Lynden-Bell, Cannon, & Godwin 1983).

In MOND, the interaction between the internal and center-of-mass motions, brought about by the theory's nonlinearity, goes beyond the Newtonian effects. For small systems (smaller than the scale over which the external field varies) the effect goes in one direction: while the center-of-mass motion is not affected by the internal motions, it may strongly affect them as explained in Bekenstein & Milgrom (1984) and Milgrom (1986). This occurs when the accelerations inside the satellite are of the order of or smaller than its center-of-mass acceleration; it is also required that the internal accelerations be small compared with the acceleration constant of MOND,  $a_0$ , as is always the case for the Milky Way's dwarf satellites. Due to this external-field effect (EFE) a satellite that plunges into the galaxy on an eccentric orbit increases in size, making itself an easier victim for tidal disruption. An additional destructive effect results when the changes in the external field become resonant with the internal motions.

The purpose of the paper is to describe, and demonstrate the pertinence, of these processes, which are peculiar to MOND.

In the next section we briefly recapitulate the external field effect. Next, in section 3, we consider a dwarf on an elongated orbit, delineating the different regimes of application of the MOND effects, and give an analytic description of dynamics in the adiabatic regime. In section 4 we describe the MOND N-body simulations, the results of which are described in section 5. Section 6 lists our conclusions and briefly comments on the Milky Way's dwarf satellites.

#### 2. The External-Field Effect

We work with the formulation of MOND as modified gravity described in Bekenstein & Milgrom (1984) whereby the Poisson equation for the nonrelativistic gravitational potential is replaced by

$$\nabla \cdot \left[ \mu(|\nabla \phi|/a_0) \nabla \phi \right] = 4\pi G \rho \tag{1}$$

(and the gravitational acceleration is given by  $-\nabla \phi$ ). For a small system, freely falling in an external field that dominates its own, equation(1) can be linearized in the internal field, expanding about the value of the external acceleration  $g_{ex}$  (approximately constant over the extent of the small system). As shown in Milgrom (1986) one gets a quasi-Newtonian internal dynamics with an effective gravitational constant  $G_e = G/\mu(g_{ex}/a_0)$ . We use the term "quasi-Newtonian" because, in addition to the increased effective gravitational constant, the dynamics is anisotropic with some dilation along the direction of the external field. If the external field is in the z direction then the linearized equation reduces to the Poisson equation in the coordinates  $x, y, z(1 + L)^{-1/2}$ , where  $L \equiv dln[\mu(s)]/dln(s)$  at  $s = g_{ex}/a_0$  takes a value between 0 and 1. In the deep-MOND limit  $[s \ll 1$ , where  $\mu(s) \approx s]$ , assumed all along in this paper, we then have

$$G_e = Ga_0/g_{ex} \gg G,\tag{2}$$

and  $L \approx 1$ .

## 3. A satellite on an elongated orbit

MOND's basic premise is that our galaxy, like others, does not contain dynamically important dark matter. Thus, as long as the orbit of the satellite under consideration does not take it within a few scale lengths of the mother galaxy, the latter may be treated as a point mass. Even within galaxies the mean accelerations never much exceed  $a_0$ ; at large galactocentric distances the acceleration is always smaller than  $a_0$ , as we assume all along. The MOND-limit acceleration at a distance R from a point mass M is

$$g(R) = V_{\infty}^2 / R,\tag{3}$$

where  $V_{\infty} \equiv (GMa_0)^{1/4}$  is the asymptotic, circular-orbit speed. This g(R) is the external acceleration field  $g_{ex}$  that enters the quasi-Newtonian internal dynamics of the dwarf on the sections of its orbit where g(R) outweighs the internal accelerations. If along some portion of the dwarf's orbit the change in the external field is slow-i.e., occurs on time scales long compared with the internal dynamical time—the quantity vr is expected to remain constant

as an adiabatic invariant. Here v is some mean internal velocity, and r is the mean radius of the system. Also, in the quasi-Newtonian regime an effective, Newtonian virial relation should hold:  $v^2 \approx G_e M r^{-1}$ . As R varies along this section of the orbit, and with it  $G_e$ , we expect v and r to follow according to  $v \propto G_e \propto R$ , and  $r \propto G_e^{-1} \propto R^{-1}$ . As the dwarf plunges in on an eccentric orbit it puffs up—an effect that does not appear in Newtonian dynamics with dark matter—thus rendering itself more susceptible to tidal breakup than it would be due to the increasing external-field gradients alone.

To consider more quantitatively the interplay between adiabaticity, external-field dominance, and tidal breakup, consider a satellite described by its gross properties: the (baryonic) mass m, the root-mean-square velocity of the constituents with respect to the center-of-mass v, and the size r (say the rms distance of constituents from the center). It moves on an orbit R(t) with velocity V(t) in the field of the point-like mother galaxy of mass M. (We neglect the secondary effects of anisotropy and so we only consider the magnitude of the position vector  $\vec{R}$ .)

The parameter

$$\beta \equiv v^2 / r g(R) = v^2 R / V_\infty^2 r \tag{4}$$

measures the importance of the internal acceleration vis-a-vis the external one. The EFE is pertinent when  $\beta \lesssim 1$ . In terms of the radii and masses we can write

$$\beta \approx \begin{cases} (R/r)(m/M)^{1/2} & \text{if } \beta \gg 1; \\ (R/r)^2(m/M) & \text{if } \beta \ll 1. \end{cases}$$
 (5)

Here we used Newtonian expressions with  $G_e$  from eq.(2) when  $\beta \ll 1$ . The parameter

$$\gamma \equiv (R/V_{\infty})/(r/v) = (R/r)^{1/2} \beta^{1/2} \tag{6}$$

is useful for measuring the degree of adiabaticity (achieved when  $\gamma \gg 1$ ) when the orbit is mildly eccentric, because then the orbital changes occur on a time scale R/V, and  $V \sim V_{\infty}$ . (The MOND potential far from a central mass is logarithmic, for which the virial relation reads  $\langle V^2 \rangle = V_{\infty}^2$ . The velocities at perigalacticon,  $V_p$ , and apogalacticon,  $V_a$ , are related by  $V_p^2 - V_a^2 = V_{\infty}^2 ln(R_a/R_p)$ , where  $R_p$  and  $R_a$  are the respective distances.) We can write

$$\gamma \approx \begin{cases} (R/r)(m/M)^{1/4} & \text{if } \beta \gg 1; \\ (R/r)^{3/2}(m/M)^{1/2} & \text{if } \beta \ll 1. \end{cases}$$
 (7)

Because only  $R \gg r$  is of interest, we see from eq.(6) that  $\gamma \gg 1$  in the whole region  $\beta > 1$ .

Tidal effects in the bulk are important when the mean internal acceleration,  $g_{in}$ , is smaller than the increment of the external acceleration over the extent r; i.e., when  $g_{in} \leq V_{\infty}^2 r/R^2 = g(R)r/R$ . We take as the criterion for the importance of tidal effects

$$\alpha \equiv [g_{in}/(V_{\infty}^2 r/R^2)]^{1/3} = (vR/V_{\infty}r)^{2/3} \lesssim 1.$$
 (8)

Again, since only cases for which  $r \ll R$  are of interest we see that tidal effects need concern us only when  $g_{in} \ll g$  ( $\beta \ll 1$ ). In this regime we have  $\alpha \approx (R/r)(m/M)^{1/3}$ . Note in general that  $\alpha = \gamma^{2/3}$ . This means that non-adiabaticity and tidal effects enter at about the same place on the orbit, as is indeed verified in our numerical calculations. Clearly, the inflation of the satellite due to the EFE continues in the tidal phase.

We can now qualitatively see what happens to a dwarf on an elongated orbit. If the entire orbit has  $\beta \gg 1$  the satellite is unaffected by the Galaxy. If its orbit takes it to a small enough galactocentric distance  $R_0$  where  $\beta = 1$  the EFE enters into action there. At this point the situation is adiabatic with  $\gamma_0 = \gamma(R_0) \approx (R_0/r_0)^{1/2}$ , which is  $\sim 10$  for the typical value of  $R_0/r_0 \sim 100$ . As R decreases further we are, at first, in the adiabatic regime with  $r \approx r_0 R_0/R$ ,  $v \approx v_0 R/R_0$ , and  $\beta$  decreasing still below 1:  $\beta \approx (R/R_0)^4$ . In this region  $\gamma \approx \gamma_0 (R/R_0)^3$  from eq.(7), so roughly at  $R = R_0 \gamma_0^{-1/3}$  adiabaticity is lost, and at the same time tidal effects set in, in which case we have to resort to MOND, N-body calculations, as described below.

The comparison of the MOND predictions on the onset of tidal effects with those of Newtonian dynamics (ND) (with dark matter) depends on what exactly is measured, and on what is assumed in ND (e.g., on the dark-matter distribution in the dwarf). But, in any event, the puffing up of a dwarf in the  $\beta \leq 1$  region, which has no analogue in ND, makes dwarfs more vulnerable to tidal disruption. To take a specific example, suppose a satellite is observed at  $R = R_1$  with measured size, internal, and center-of-mass velocities. Its future orbit can then be deduced, and also the Newtonian, dynamical mass it contains,  $m_N$ . Suppose it is already in the  $\beta \leq 1$  regime. It is easy to see that the value of its tidal parameter  $\alpha$  as deduced in ND is the same as that given by MOND, since  $m_N = mG_e(R_1)/G$  and the galactic mass within  $R_1$  is  $M_N(R_1) = MG_e(R_1)/G$ . As we saw, MOND predicts that  $\alpha \propto R^2$ , while Newtonian dynamics predicts  $\alpha \propto R^{2/3}$ , since r is then assumed to remain constant while  $M_N(R) \propto R$ . So tidal effects will clearly enter at larger radii in MOND.

## 4. N-body simulations

The numerical simulations involve a model dwarf comprising N identical particles that starts with some equilibrium distribution function in compliance with MOND dynamics. The model is then subjected to different types of variable external influences that mimic aspects of the influence of the mother galaxy. The underlying potential field equation is eq.(1), or its linearized, approximate form. This nonlinear potential equation is solved

numerically using multi-grid methods as detailed in Brada (1996) and adumbrated in Brada & Milgrom (1999). The particles are then propagated in the derived potential. It is only interesting to study the dwarf when it is in the external-field-dominated region. To isolate the different effects discussed above we proceed in three steps. First, to pinpoint the effects of non-adiabaticity, and verify our analytic deductions for the adiabatic regime, we start with a quasi-Newtonian King model for the dwarf, assume quasi-Newtonian dynamics, and simply vary  $G_e$  periodically and see how the model reacts for different frequencies of the perturbation. In the second step we still consider a quasi-Newtonian behavior but the applied variations in  $G_e$  and the direction of the external field correspond to actual orbits of a dwarf. The third stage, which is more costly, is to simulate the complete system of dwarf plus a point-mass galaxy. Since the construction of initial models for the dwarf are peculiar to MOND we describe them briefly now, referring the reader for more details to Brada (1996).

## 4.1. Constructing steady-state galactic models

We use as initial states King models (For details see, e.g., Binney & Tremaine 1987) properly modified to constitute, as the case may require, quasi-Newtonian or deep-MOND steady states. The distribution function for the Newtonian models is

$$f_K = \begin{cases} \rho_1 (2\pi\sigma^2)^{-3/2} (e^{\varepsilon/\sigma^2} - 1) & \text{if } \varepsilon > 0\\ 0 & \text{if } \varepsilon \le 0, \end{cases}$$
 (9)

where  $\varepsilon \equiv -E + \phi_0$ ,  $E = v^2/2 + \phi$ , and the parameter  $\phi_0$  is the upper energy cutoff. Equation(9) is integrated over velocities to obtain the density  $\rho_K(\Psi)$  as a function of the relative potential  $\Psi \equiv -\phi + \phi_0$ . Instead of the Poisson equation we solve here the spherically symmetric MOND equation (in the deep-MOND limit assumed all along):

$$[a_0^{-1}r^2(\Psi')^2]' = -4\pi G\rho_K(\Psi) \tag{10}$$

(the apostrophe signifies derivative with respect to r), which provides an ordinary differential equation for  $\Psi(r)$  that can be integrated numerically with the boundary condition  $\Psi'(0) = 0$ . The second boundary condition is  $\Psi(0)$ , which together with  $\phi_0$  determines the model. The model can also be specified in terms of other parameters from among the tidal radius  $r_t$ , the total mass, the central density  $\rho(0)$ , and the King radius  $r_0 \equiv (9\sigma^2/4\pi G\rho_0)^{1/2}$ . Note that for MOND King models  $r_0$  defined in this way is not some characteristic radius; it is just a convenient representation of  $\rho_0$  (so we can have  $r_0 > r_t$ , for example).

In constructing a quasi-Newtonian model we remember that the transformed potential  $\phi'(x',y',z') \equiv \phi(x,y,z)$ , with  $x'=x,\ y'=y,\ z'=z(1+L)^{-1/2}$ , with  $L=dln[\mu(s)]/dln(s)$ , satisfies the usual Poisson equation with  $G_e$  as gravitational constant, and  $\rho'(x',y',z') \equiv \rho(x,y,z)$  as density (z is taken in the direction of the external field). We thus begin by constructing a Newtonian model in the auxiliary coordinates  $x',\ x',\ z'$  remembering that the conserved quantity on which the distribution function depends by the Jeans theorem is  $[v_x'^2+v_y'^2+(1+L)v_z'^2]/2+\phi'(x',y',z')$ . This model has a spherical mass distribution, but a  $v_z'$  dispersion that is smaller by a factor  $(1+L)^{1/2}$  than those in the other directions. We draw positions and velocities for the auxiliary coordinates of the N particles. Then we multiply all z' and  $v_z'$  values by  $(1+L)^{1/2}$ . The total mass of the model is multiplied by the same factor because  $\int \rho'(\vec{r}')d^3r' = (1+L)^{-1/2}\int \rho(\vec{r})d^3r$ . The resulting model is elongated in the z direction and has an isotropic global velocity distribution.

#### 5. Results of the simulations

## 5.1. Testing for the external-field effect

We first want to establish the consequences of the external-field effect and learn what is the time scale necessary for a change to be adiabatic. As was discussed in section 3., in the adiabatic regime we expect the average velocity in a system, v, to be proportional to  $G_e = G(a_0/g_{ex})$ , and the average size of the system to be inversely proportional to  $G_e$ . We start with a Newtonian King model having  $10^5$  particles with  $\sigma^2 = 1$ ,  $r_0 = 1$ , and  $\Psi(0)/\sigma^2=1$ . We also take G=1 [this fixes  $\rho(0)$ ; the total mass of the Newtonian model is then m = 0.72, and its tidal radius  $r_t = 1.975$ ]. We then perform the stretching by  $2^{1/2}$  (we take L=1 for the deep-MOND limit) to get a model with m=1.02 and root-mean-square values of the coordinate and velocity components (designated by capital letters) X = Y = 0.44, Z = 0.62,  $V_x = V_y = V_z = 0.39$ . The natural dynamical time r/vis of order unity. We ran simulations on a cubical grids with  $129^3$  grid points using the quasi-Newtonian field equation with a fixed time step dt = 0.04 for  $10^3$  time steps. We varied  $G_e$  periodically with time taking  $G_e(t) = (0.7 + 0.3 \cos \omega t)^{-1}$  for three values of  $\omega = 2\pi(1/40, 1/20, 1/10)$ . (The physical grid spacing is changed in proportion to  $G_e^{-1}$ during the simulation, since we expect r to scale as  $G_e^{-1}$ .) In analogy with the adiabaticity parameter,  $\gamma$ , defined locally on an orbit, we can define here as some global measure of adiabaticity  $\hat{\gamma} \equiv (T/4)/[X(0)/V_x(0)]$ , where  $T = 2\pi/\omega$  is the period. For the three models presented  $\hat{\gamma} = 10, 5, 2.5$  respectively. The results of these simulations for the x components are shown in figure (1) describing how the extent and velocity dispersion in the x direction vary with time. The results for the z direction are the same within a few percents. The results for  $\omega = 2\pi/40$  show the expected external-field effect with strict adiabaticity; small departures from adiabaticity appear in the time dependence of the size and mean velocity for  $\omega = 2\pi/20$ ; while for  $\omega = 2\pi/10$  clear departure from adiabaticity is evident.

We also learn that departure from adiabaticity brings about a secular increase in the radius and decrease in the internal velocities.

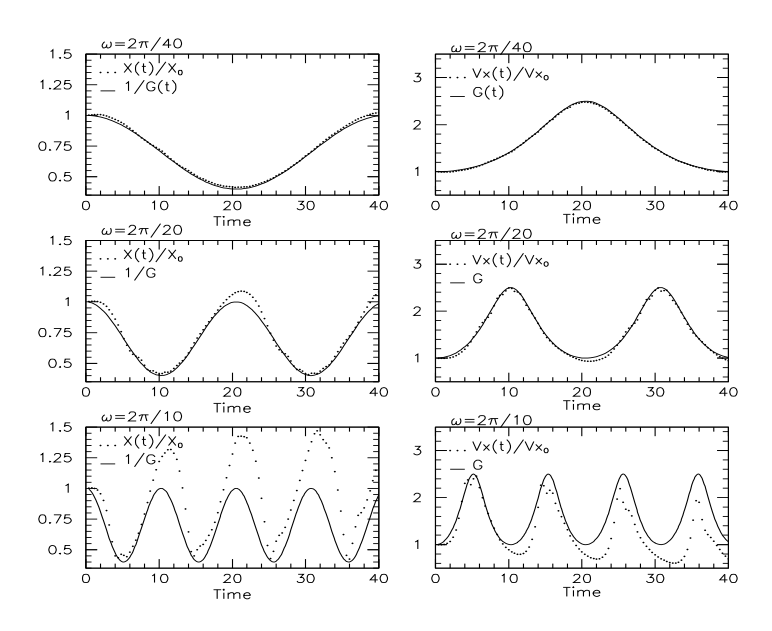


Fig. 1.— The time dependence of X(t)/X(0) and  $G_e(t)^{-1}$  (left-hand panels), and  $V_x(t)/V_x(0)$  and  $G_e(t)$  (right-hand panels) for a quasi-Newtonian King model with  $m=1.02, X(0)=0.44, V_x(0)=0.39$  and  $G_e=(0.7+0.3\cos\omega t)^{-1}$ . The quantities plotted in each panel should be equal for strict adiabaticity. The values of  $\omega$  are marked.

## 5.2. The evolution of a quasi-Newtonian model along a realistic orbit

Before going to the more complete models that utilize the full MOND field equation and include the tidal forces, we follow the evolution of a quasi-Newtonian model varying the value of  $G_e$  and the direction of the external field according to the location of the dwarf on an actual orbit in the logarithmic potential of the point-mass mother galaxy. Tidal forces are then not taken into account. The purpose of these experiments is to test

the degree to which the changes in dwarf characteristics are adiabatic for sample models with realistic parameters. In particular, to see what lasting effects non-adiabaticity near perigalacticon has on the dwarf in disjunction from tidal effects. We thus took orbits with strong adiabaticity at apogalacticon, where we start, but a breakdown of adiabaticity near perigalacticon. Note that  $G_e$  goes back to the same value at subsequent apogalacticons; so, apart from some remaining oscillations on the dynamical time scale, the virial relation is reestablished in the mean, and, thus,  $v^2r$  must come back to the same value.

We take the mass of the mother galaxy as unit, M=1. Since we also use units in which G=1 and  $a_0=1$ , the unit of velocities becomes  $V_{\infty}\equiv (MGa_0)^{1/4}=1$ , which in cgs units is about  $220kms^{-1}$  for the MW. Length is then measured in units of  $V_{\infty}^2/a_0$ , about 10 kpc for the MW. In these units the MW satellites are typically at distances between 5 and 20, of size  $3\times 10^{-2}$  to  $10^{-1}$ , velocity dispersion  $2\times 10^{-2}$  to  $5\times 10^{-2}$ , and of mass  $10^{-5}$  to  $10^{-4}$ . Accordingly, we construct our dwarf model as a quasi-Newtonian King model having the following properties:  $\sigma^2=8\times 10^{-4}$ ,  $r_0=1/16$ ,  $\Psi(0)/\sigma^2=1$ ,  $r_t=0.1234$  (before stretching), and  $m=5.09\times 10^{-5}$ . We simulated its evolution for two orbits with pericenter and apocenter distances of  $R_{min}=6$ ,  $R_{max}=9$ , and  $R_{min}=6$ ,  $R_{max}=12$ . At galactocentric distance R the external acceleration is  $R^{-1}$  (in our units of  $a_0$ ), and  $G_e=R$ .

The results of the simulations are summarized in figures (2)(3). Adiabaticity is more severely violated in the second model, which has  $R_{max} = 12$ . We see that, as a result of violating adiabaticity near  $R = R_{min}$ , the dwarf still oscillates on the dynamical time scale when it next enters the adiabatic regime around apocenter. More importantly, it attains a larger radius (averaged over the fluctuations). The velocity dispersion is correspondingly smaller ( $v^2r$  is preserved and vr is larger). On the next close passage the dwarf will be even less adiabatic and becomes more vulnerable and will continue to increase in size.

## 5.3. The evolution of a full MOND model along a realistic orbit.

We then followed the full evolution of a dwarf obeying MOND orbiting a point mother galaxy. We started by producing an isolated MOND King model with the following parameters:  $\sigma^2 = 8.53 \times 10^{-3}$ ,  $r_0 = 0.3$  (remember that  $r_0$  is just a proxy for  $\rho_0$ , not a characteristic radius), and  $\Psi(0)/\sigma^2 = 1$ . The resulting model has a total mass  $m = 3.59 \times 10^{-5}$  and a tidal radius  $r_t = 0.1346$ . Note that  $\sigma$  is not the mean velocity dispersion of the MOND model. This can be gotten from the deep-MOND virial relation (Milgrom 1994), which in our units reads  $\langle v^2 \rangle = 2m^{1/2}/3$ , where  $\langle v^2 \rangle$  is the three-dimensional rms velocity. So we get for the one-dimensional rms velocity  $\langle v_x^2 \rangle = 1.33 \times 10^{-3}$ .

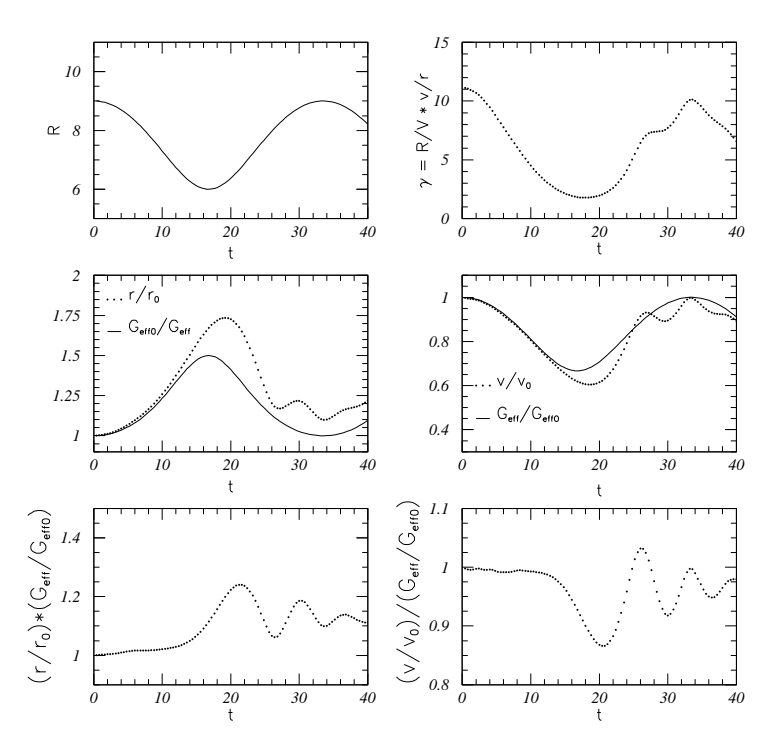


Fig. 2.— Orbital and intrinsic parameters as functions of time for a dwarf subject to an EFE. The field varies as it would on an orbit with  $R_{max}=9\ R_{min}=6$  (tidal effects are excluded).

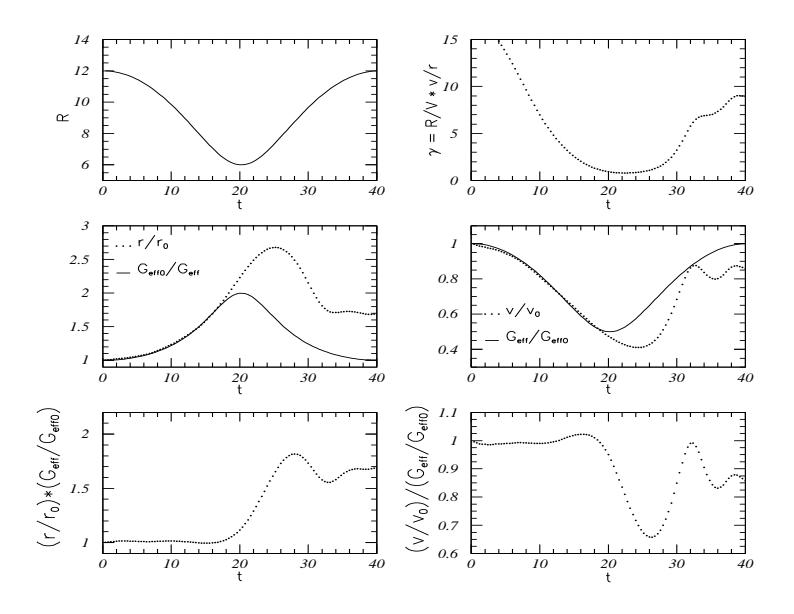


Fig. 3.— Same as figure 2 for  $R_{max} = 12$  and  $R_{min} = 6$ .

These global parameters are similar to the ones of the quasi-Newtonian model we have used in the previous subsection, but the density profiles of the two models differ: the MOND model is less concentrated than the quasi-Newtonian model. Our model dwarf is put on an eccentric orbit starting at an apogalacticon distance of  $R_{max} = 12$  and reaching a perigalacticon distance of  $R_{min} = 6$ . From the above model we construct a family of five models by scaling up the mass of the model ending up with masses m, 2m, 3m, 4m, and 16m, and scaling the velocity dispersions up accordingly. These are all models for isolated MOND dwarfs. However, at apocenter already we have to start with models under some external-field influence. So, before we let the models evolve along the orbit we need to switch on adiabatically the external field. This is done in a preliminary simulation where we gradually increase the mass of the mother galaxy from zero to one.

The presence of the mother galaxy enters these simulations through the boundary conditions used by the potential solver. The 16m model hardly changes when the external field is switched on, while for the m model the rms radius, r, increases by as much as 50% when the external field is switched on. The values for the parameter  $\beta$ , which measures the ratio of the internal field to the external field, calculated at R=12 are 0.233, 0.7, 1.03, 1.29, and 3.09, respectively. Thus, the m model is dominated by the external field while the 3m is the borderline case. We then integrate the internal dynamics and the center-of-mass motion of each of the models on the orbit. The orbits lie in the X,Y plane and we start at Y=12, X=0. The simulations lasted for 40 time units and consisted of  $10^3$  individual time steps. The rms value of r and v as functions of time are given in figure (4). Also shown there are the adiabaticity ( $\gamma$ ) and the tidal ( $\alpha$ ) parameters along the orbit. Projections of the dwarf structure for the four smaller-mass models, on the X-Y plane, are given in figure (5).

The value of the parameter  $\beta$  at pericenter for the five models was: 0.0315, 0.056, 0.168, 0.2106, and 1.36, respectively. The three models with masses m, 2m and 3m show clear signs of tidal disruption. The m model seems to have been totally destroyed by the tidal forces and there is no clear core that remained after the passage near the galaxy. The 2m model was strongly influenced by the tidal forces and lost about 25% of its mass. The 3m model lost only a few percent of its mass through tidal interaction. We can attribute these mass losses to the combined action of tidal forces and the extra non-adiabatic expansion of the models near  $R = R_{min}$ .

In comparison, Newtonian dynamics applied to dwarfs observed with the same initial positions, center-of-mass velocities, sizes, and velocity dispersions would predict much less tidal disruption. Consider, in particular, the two most vulnerable models with masses m and 2m. They start at R=12 with  $\beta<1$ , so, from the discussion at the end of section

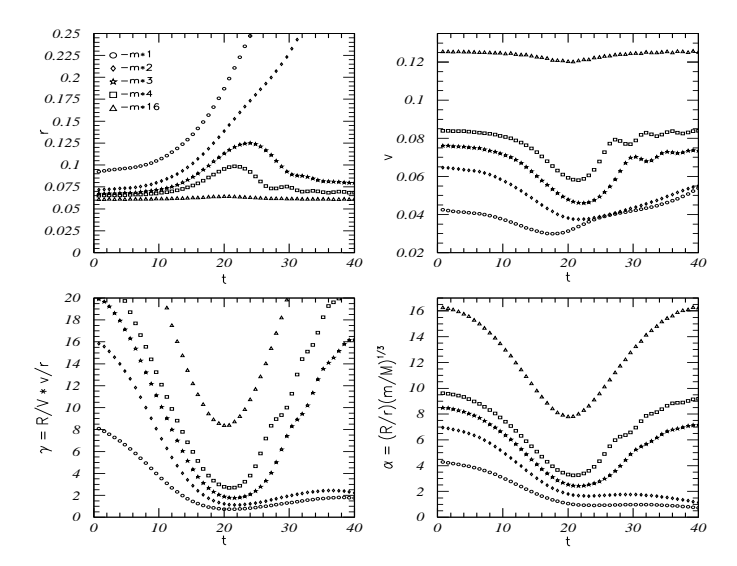


Fig. 4.— Dwarf parameters as functions of time for five dwarf masses for the full model calculation, all starting at apocenter at R = 12 and reaching pericenter at R = 6.

3 we see that their Newtonian  $\alpha$  values there are the same as the MOND values. (Of course, a Newtonist will assume that they contain more mass for the same sizes and velocity dispersions.) From figure 4 we see that the two models start with  $\alpha \approx 4$ , 7 respectively. The MOND scaling ( $\alpha \propto R^2$  for  $\beta \ll 1$ ) implies that the two models should have  $\alpha \approx 1, 1.7$  at perigalacticon, R=6, as they approximately do. In Newtonian dynamics, where  $\alpha \propto R^{2/3}$ , we would get at perigalacticon  $\alpha \approx 2.5, 4.4$  for the two models, making these initial model dwarfs much safer from later tidal disruption. It need perhaps be clarified that the Newtonist will continue to get the same  $\alpha$  values as in MOND if he uses at every point the observed properties, but this will lead him to conclude that the mass of the dwarf varies. Here we speak of what the Newtonist's predictions will be given only the initial data, and assuming that the dwarf mass is constant.

## 6. Summary and conclusions

We have studied the existence, the nature, and the influence on dwarf satellites of the external field effect in MOND. For dwarf parameters in the EFE regime two situation are grossly distinguished: a) the adiabatic regime, in which tidal effects are not so important and b) the impulsive region, which also roughly coincides with the region where tidal

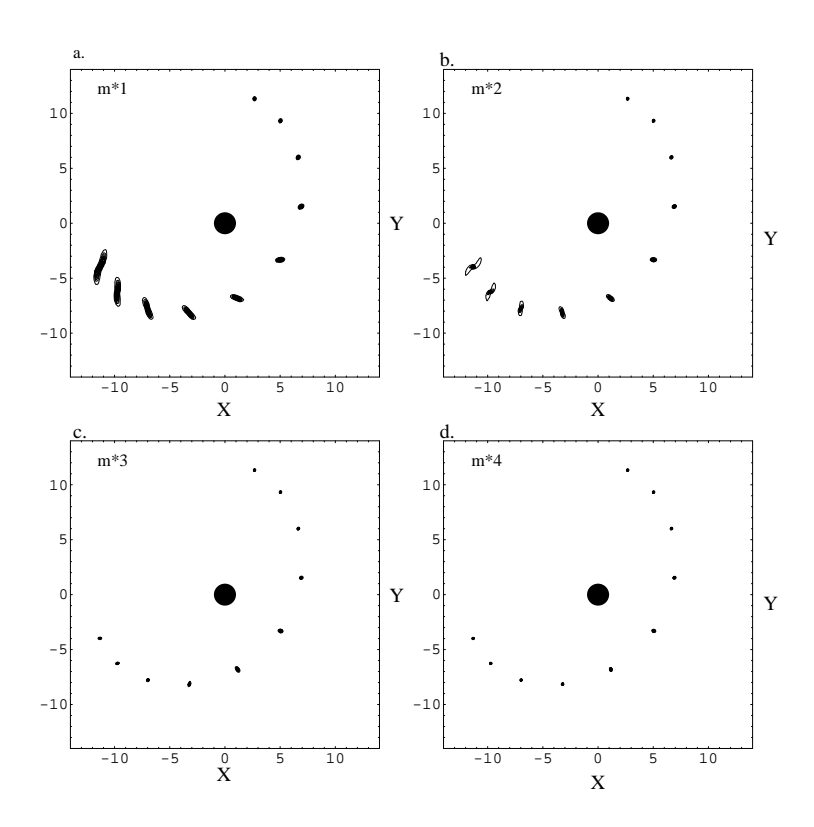


Fig. 5.— Projection of the mass on the X-Y plane for the 1m (a), 2m (b), 3m (c), and 4m (d) models. The mother galaxy is represented by the dark disk. Snapshots are taken every 4 time units (about every  $2 \times 10^8$  years for the MW).

forces become important. Due to the EFE the radius of a dwarf in the adiabatic regime increases as it approaches the mother galaxy. If the whole orbit is in the adiabatic regime, the structure of the dwarf simply changes periodically with the orbital period. If, however, some segment of the orbit is in the impulsive-tidal regime near pericenter, then the dwarf might lose much of its mass there. Even if it does not, it can emerge from this region having a larger radius and smaller velocity dispersion (hence, a longer intrinsic dynamical time). In its next approach to perigalacticon it will thus enter the impulsive-tidal regime at a larger distance from the center.

Clearly, all the above is highly germane to the dwarf system of the MW. The distribution of intrinsic and orbital parameters of presently observed dwarfs must have been greatly affected by interaction with the MW. And, one expects, MOND would give a different answer than Newtonian dynamics with dark matter. To actually deduce the present-day properties of the dwarfs would, however, require knowledge of the initial distribution of the orbital and intrinsic parameters of the dwarf-satellite population. Nothing is really known about this, so we refrain from speculating on the subject. We only estimate where our dwarf satellites stand as regards external-field dominance, adiabaticity, and the importance of tidal effects.

We consider the 10 dwarf spheroidal satellites with known parameters (Mateo 1998): Sculptor, LSG 3, Fornax, Carina, Leo I, Sextans, Leo II, Ursa Minor, Draco, and Sagittarius. We take for the MW  $V_{\infty} = 220 \text{ kms}^{-1}$ . Since only core radii,  $r_c$ , are given we write for the mean radius  $r = \eta r_c$  to get for the adiabaticity parameter of those dwarfs  $\gamma \sim \eta^{-1}(22, 150, 14, 15, 47, 8, 39, 14, 20, 2)$ , respectively. So, with the exception of Sagittarius—which is known to be in the throes of disruption—and perhaps Sextans, these dwarfs are in the adiabatic regime within reasonable margins for  $\eta$ , and even considering the approximate nature of the  $\gamma$  criterion. According to our analysis they are also only weakly affected by tidal forces at their present positions. As has been pointed out (Milgrom 1995, McGaugh & de Blok 1998), most of the above dwarfs (with the exception of LSG 3, Leo I, and Leo II) are materially affected by the EFE: with the above choices of system parameters we get  $\beta \sim \eta^{-1}(0.7, 4.4, 0.7, 0.5, 1.9, 0.2, 1.2, 0.6, 0.9, 0.1)$ .

If we apply the MOND scaling  $\alpha \propto R^2$ , which is valid in the  $\beta \ll 1$  regime, to the dwarfs with  $\eta\beta < 1$  (except for Sagittarius) we can estimate the minimum galactocentric distance above which the bulk of the dwarf is immune to tidal effects. This is given by  $R_t^M \approx R_0 \alpha_0^{-1/2} = R_0 \gamma_0^{-1/3}$ , where here a subscript 0 marks present-day values. (If a dwarf in now on an outgoing section of its orbit it will return to the same R, as it goes in, in the same state.) For Sculptor, Fornax, Carina, Sextans, UMi, and Draco we get, respectively  $R_t^M \sim \eta^{1/3}(28, 57, 41, 43, 27, 32)$  kpc. The corresponding Newtonian values  $(R_t^N \approx R_0 \gamma_0^{-1})$ 

are  $R_t^N \sim \eta(4, 10, 7, 11, 5, 4)$  kpc. They are smaller than the corresponding MOND values if  $\eta$  is not so large that  $\alpha_0 < 1$ . (For some dwarfs these Newtonian radii may fall within the stellar MW where our approximation of a spherical, logarithmic potential is not valid.)

Our results imply that for a given dwarf in the adiabatic regime on an elongated orbit under a strong EFE the size and velocity dispersion would be strongly dependent on the distance from the mother galaxy. One might then try to look for such correlations in the time-frozen population as seen today. This seems to us quite hopeless at present because the effects will be swamped by other factors of which we know very little; in particular, the unknown distribution of initial (intrinsic and orbital) parameters for the dwarfs. This is aggravated by the small sample size.

We leave for a future publication some other interesting effects predicted by MOND that result from the EFE. For example, in a dwarf in the EFE regime the total angular momentum is not conserved. We alluded to the fact that the direction of the external field if felt by the "internal" dynamics of the dwarf. In a static or adiabatic situation only the angular momentum along the external-field direction is conserved.

We thank the referee, Tad Pryor, for many useful comments and suggestions

#### REFERENCES

Aaronson, M., & Olszewski, E.W. 1988, in IAU Symposium 130 Large Scale Structure of the Universe, J. Audoze, M.C. Pelletan, & A. Szalay Eds (Dordrecht, Kluwer Academic Press)

Bekenstein, J., & Milgrom, M. 1984, ApJ, 286, 7

Binney, J., & Tremaine, S. 1987, Galactic Dynamics, Priceton University Press

Brada, R. 1996, PhD thesis, Weizmann Institute

Brada, R., & Milgrom, M. 1999, ApJ, 519, 590

Faber, S.L., & Lin, D.N.C. 1983, ApJL, 266, L17

Little, B., & Tremaine, S. 1987, ApJ, 320, 493

Lynden-Bell, D., Cannon, R.D., & Godwin, P.J. 1983, MNRAS, 204, 87p

Mateo, M.L. 1998, ARA&A, 36, 435

McGaugh, S., & de Blok, W.J.G. 1998, ApJ, 499, 66

Milgrom, M. 1986, ApJ, 302, 617

Milgrom, M. 1994, ApJ, 429, 540

Milgrom, M. 1995, ApJ, 455, 439

Pryor, C. 1991, proceedings of the OAC Fifth International Workshop, Morphological and Physical Classification of Galaxies, G. Busarello, M. Capaccioli, & G. Longo, eds. Kluwer Publ. Co.

This preprint was prepared with the AAS  $\mbox{\sc IAT}_{\mbox{\sc E}}\mbox{\sc X}$  macros v3.0.